

ViLU: Learning Vision-Language Uncertainties for Failure Prediction

Marc Lafon^{*†1} Yannis Karmim^{*1} Julio Silva-Rodriguez³ Paul Couairon²
 Clément Rambour^{1,2} Raphaël Fournier-Sniehotta^{1,2} Ismail Ben Ayed³ Jose Dolz³
 Nicolas Thome²

¹Conservatoire National des Arts et Métiers, CEDRIC, F-75141 Paris, France

²Sorbonne Université, CNRS, ISIR, F-75005 Paris, France

³ETS Montreal, Canada

Abstract

Reliable Uncertainty Quantification (UQ) and failure prediction remain open challenges for Vision-Language Models (VLMs). We introduce ViLU, a new Vision-Language Uncertainty quantification framework that contextualizes uncertainty estimates by leveraging all task-relevant textual representations. ViLU constructs an uncertainty-aware multi-modal representation by integrating the visual embedding, the predicted textual embedding, and an image-conditioned textual representation via cross-attention. Unlike traditional UQ methods based on loss prediction, ViLU trains an uncertainty predictor as a binary classifier to distinguish correct from incorrect predictions using a weighted binary cross-entropy loss, making it loss-agnostic. In particular, our proposed approach is well-suited for post-hoc settings, where only vision and text embeddings are available without direct access to the model itself. Extensive experiments on diverse datasets show the significant gains of our method compared to state-of-the-art failure prediction methods. We apply our method to standard classification datasets, such as ImageNet-1k, as well as large-scale image-caption datasets like CC12M and LAION-400M. Ablation studies highlight the critical role of our architecture and training in achieving effective uncertainty quantification. Our code is publicly available and can be found here: [ViLU Repository](#).

1. Introduction

Vision Language Models (VLMs) [9, 25, 27, 36, 50] are highly popular foundation models pre-trained on large-scale image-text datasets, e.g., LAION [37]. They possess the appealing capability of performing zero-shot image classification, meaning they can classify samples into classes that

were not seen during training.

Uncertainty quantification (UQ) is a fundamental challenge in deep learning and involves estimating the confidence of a model’s predictions. This paper addresses the problem of reliable UQ for VLMs to detect their potential failures in downstream tasks. Reliable UQ is crucial in safety-critical domains and offers significant opportunities for various applications involving VLMs, such as failure prediction [17], out-of-distribution detection [46], active learning [47], and reinforcement learning [12], among others.

The vanilla method for UQ with VLMs is the Maximum Concept Matching (MCM) score [30], a direct extension of Maximum Class Probability (MCP) [17] for classification. Although MCM is a strong baseline, it suffers from fundamental drawbacks: by design, it assigns high confidence to failures and struggles with fine-grained concepts. As illustrated in Fig. 1, the VLM misclassifies the “Eskimo dog” image as a “Siberian husky”, and the high MCM score prevents the detection of the error.

In classification, learning-based methods have also been explored for failure prediction. In particular, a few deep learning models designed to predict the classifier’s loss and dedicated to learning visual uncertainties (LVU) have been proposed [8, 19, 47]. However, when applied to VLMs, these methods do not model the relationships between downstream concepts, intrinsically limiting their failure prediction performance. The example in Fig. 1 still receives a high confidence score with LVU methods. Furthermore, although recent methods have proposed specific calibration techniques for VLMs [31, 34, 42, 44, 48], fewer works have focused on UQ solutions for VLMs in general, with the exception of the recent [2].

This paper introduces ViLU, a post-hoc framework for learning Vision-Language Uncertainties and detecting VLMs’ failure. The core idea in ViLU is to define a confidence score depending both on the visual input but also on the set of concepts that defines the downstream task,

[†] Corresponding author: marc.lafon@lecnam.net

^{*} Equal contribution

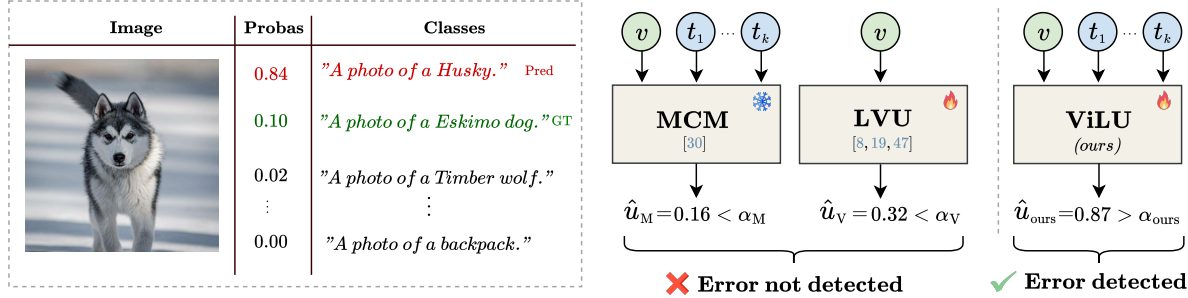


Figure 1. **Motivation of ViLU.** In zero-shot classification with VLMs, uncertainty may arise from both the image and target concept definitions. Given an ambiguity between several concepts, the vanilla Maximum Concept Maxing (MCM) [30], can assign a high confidence to a wrong prediction, *e.g.* a "Eskimo dog" wrongly classified as a "Siberian husky". Previous methods based on Learning Visual Uncertainties (LVU) [8, 19, 47] do not account for ambiguity between concepts and often fail, whereas ViLU captures a fine-grained uncertainty by contextualizing the image within the spectrum of possible textual concepts.

e.g. classification or caption matching. By finely modeling the interaction between the image and the target concepts, ViLU assigns a low confidence score to the misclassified example – see Fig. 1.

We summarize our key contributions as follows:

- ViLU introduces a novel multi-modal uncertainty representation that integrates visual embeddings, predicted textual embeddings, and image-conditioned textual representations via a cross-attention module. This formulation enables the model to capture fine-grained ambiguities between the input image and candidate concepts, significantly improving failure prediction.
- We propose a dedicated uncertainty predictor that operates on this enriched representation and is trained to discriminate between correct and incorrect predictions using weighted binary cross-entropy (BCE). Unlike conventional loss-prediction-based UQ methods, ViLU is fully loss-agnostic, making it particularly well-suited for post-hoc uncertainty estimation in black-box VLMs.

We conduct an extensive experimental validation of ViLU on various downstream classification datasets, as well as image-caption datasets such as CC12M and LAION-400M. First, we highlight that state-of-the-art methods struggle to outperform the MCM baseline, illustrating the difficulty of the task. In contrast, ViLU delivers significant and consistent improvements over multiple baselines, including recent VLM-specific methods [2]. Thorough ablation studies further validate our architectural choices and training design for optimal performance.

2. Related Work

Vision-language models (VLMs) have gained popularity for aligning image and text representations [9, 25, 27, 36, 50], achieving unprecedented zero-shot performance by jointly learning a shared vision-text embedding space on large-scale web datasets [9, 24, 37]. They have been applied in a plethora of domains including image classification

[22, 52, 54], open-vocabulary segmentation [23, 43, 49, 51] and cross-modal retrieval [1, 18]. Nevertheless, VLMs align deterministic text and image representations without accounting for uncertainty in zero-shot predictions [2, 42]. While simple uncertainty quantification methods exist, *e.g.* MCM [30], a robust approach for failure prediction remains lacking. We address this gap with an effective UQ method for failure prediction of VLMs.

Uncertainty quantification (UQ) for failure prediction.

In classification, MCP [17] is the vanilla method for UQ. However, by only considering the maximum over the predicted probabilities, MCP tends to overestimate confidence in failure cases [8]. Another common approach is to use the Shannon entropy of the predicted softmax distribution [38], but its invariance to label permutations [14, 38] limits its effectiveness for failure detection. Recently, Doctor [14] was proposed to refine the Shannon entropy [38] using Rényi entropy, while Rel-U [13] further extended it by incorporating a learned distance matrix to model class relationships from classifier predictions. Such methods, however, suffer from a limited expressiveness in their UQ models, and struggle to capture finer-grained uncertainties. Another line of work is to learn the classifier’s loss using deep neural networks [8, 19, 47]. [47] estimates model loss to improve active learning, while [8] learns the cross-entropy loss for classification and segmentation. More recently, [19] applies this approach for large-scale UQ with vision transformers. However, these methods are limited to learning visual uncertainties (LVU), and generalize poorly to VLMs as they do not account for ambiguity in the language modality. To overcome this limitation, we propose an efficient UQ method for frozen, pre-trained VLMs and show that directly predicting failures outperforms loss prediction.

VLMs’ UQ. MCP can be easily adapted for UQ of VLMs by leveraging their zero-shot probabilities, leading to the Maximum Concept Matching (MCM) method [30]. However, MCM inherits MCP’s limitations for failure predic-

tion, especially its overconfidence for errors. However, VLMs’ overconfidence is generally less pronounced than for standard classifiers [29, 41]. As a result, when the VLM’s downstream accuracy is sufficiently high, MCM remains a strong baseline for failure prediction. Several works extend VLMs for UQ in cross-modal retrieval tasks [5, 6, 26, 32], often by learning probabilistic embeddings for each modality. However, most require retraining both visual and textual backbones, limiting their practicality [5, 6]. To address this, ProbVLM [42] learns distribution parameters over embeddings via adapters, but overlooks cross-modal similarity scores, which limits its effectiveness for failure prediction. BayesVLM [2] applies a Laplace approximation to model uncertainty over similarities post-hoc. While both capture vision-language uncertainty, their objectives are not tailored for failure prediction, which limits their performance compared to our approach.

3. Background

3.1. Contrastive vision-language models

Zero-shot predictions. Consider a particular dataset $\mathcal{D} = \{(\mathbf{x}_i, t_i)\}_{i=1}^N$, where each image $\mathbf{x}_i \in \mathcal{X}$ is paired with a class name or caption $t_i \in \mathcal{T}$. Contrastive VLMs are composed of a pre-trained vision encoder $f_V(\cdot)$ that maps an input image \mathbf{x}_i to a visual embedding $\mathbf{z}_{v_i} = f_V(\mathbf{x}_i) \in \mathbb{R}^d$, and a text encoder $f_T(\cdot)$ that embeds a textual input t_j into a representation $\mathbf{z}_{t_j} = f_T(t_j) \in \mathbb{R}^d$. This multi-modal joint embedding space is learned during pre-training by aligning paired concepts. Thus, it enables zero-shot image classification, by computing the probability $p(t_j|\mathbf{x}_i)$ of image \mathbf{x}_i being associated to caption t_j using the softmax of the similarities between the visual representations \mathbf{z}_{v_i} and the embeddings \mathbf{z}_{t_j} of a set of K candidate textual concepts:

$$p(t_j|\mathbf{x}_i) = \frac{\exp(\mathbf{z}_{v_i}^\top \mathbf{z}_{t_j} / \tau)}{\sum_k \exp(\mathbf{z}_{v_i}^\top \mathbf{z}_{t_k} / \tau)} \quad (1)$$

where τ is a temperature parameter optimized during pre-training, and \mathbf{z}_{v_i} and \mathbf{z}_{t_j} are ℓ_2 -normalized embeddings.

3.2. VLMs’ failure prediction with MCM

We aim to determine whether VLMs can recognize when their predictions are unreliable. This is captured by an uncertainty scoring function, $u(\mathbf{x})$, where higher values indicate a greater likelihood of misclassification.

Maximum Concept Matching (MCM) [30] corresponds to the probability of the predicted caption for image \mathbf{x}_i , *i.e.*, the one with the highest probability:

$$u_{\text{MCM}}(\mathbf{x}_i, \mathbf{t}_1, \dots, \mathbf{t}_k) = 1 - \max_j p(\mathbf{t}_j|\mathbf{x}_i). \quad (2)$$

Limitations. Despite being a reasonable UQ method in coarse-grained classification tasks, u_{MCM} has fundamental limitations. Firstly, the max operation in Eq. (2) by

design assigns an overestimated UQ for incorrect predictions. Therefore, MCM performances drop when the zero-accuracy of the classifier is low, as shown in the experiments. Also, in fine-grained classification or open-vocabulary settings, visual and textual alignments become more dispersed, reducing MCM’s reliability. This limitation is particularly problematic for modern VLMs, which are trained on large-scale datasets for open-vocabulary tasks.

4. ViLU model

This section presents our ViLU framework for multi-modal failure prediction on VLMs, as illustrated in Fig. 2. We first introduce our general post-hoc methodology in Sec. 4.1, which enables UQ on VLMs without modifying their internal parameters. We then describe our architecture in Sec. 4.2, detailing the design of ViLU’s embedding using image-text cross-attention, and of our failure classification head. Finally, we outline ViLU’s training procedure in Sec. 4.3, including our weighted cross-entropy loss that directly aligns with the failure prediction task.

4.1. Methodology for UQ on VLMs

Post-hoc Setting. We aim to design a discriminative and reliable UQ measure for pre-trained VLMs. To achieve this, we adopt a post-hoc approach, relying solely on visual and textual representations, *i.e.*, $\mathcal{D} = \{(\mathbf{z}_{v_i}, \mathbf{z}_{t_i})\}_{i=1}^N$. This allows the UQ model to be easily integrated on top of a pre-trained VLM, providing uncertainty estimates without modifying internal representations, requiring fine-tuning, or depending on the loss function used during training.

Learning vision-language uncertainties. We propose leveraging the interactions between the *visual modality* and the *set of candidate concepts* to estimate uncertainty for failure prediction. Uncertainty in model predictions can arise from *visual patterns* (*e.g.*, low image quality, ambiguous features) or *textual patterns*, which define concept distinctions. Additionally, it is shaped by cross-modal interactions. To model these interactions, we learn a global uncertainty representation $u_\theta(\cdot)$ that captures visual-textual interactions and their inherent uncertainty. We adopt a *data-driven approach*, training the uncertainty module to predict VLMs’ misclassifications. Specifically, we frame our objective as a *binary classification task*, where u_θ predicts whether an input will be misclassified by the VLM (see Sec. 4.3). Formally, let us define our uncertainty module as:

$$u_\theta : \quad \begin{array}{ccc} \mathbb{R}^d \times \mathbb{R}^{K \times d} & \rightarrow & [0, 1] \\ (\mathbf{z}_v, \mathbf{z}_{t_1}, \dots, \mathbf{z}_{t_K}) & \rightarrow & u_\theta(\mathbf{z}_v, \mathbf{z}_{t_1}, \dots, \mathbf{z}_{t_K}) \end{array} \quad (3)$$

Note that our uncertainty function in Eq. (3) can handle varying values of K , as the number of candidate concepts may vary during inference.

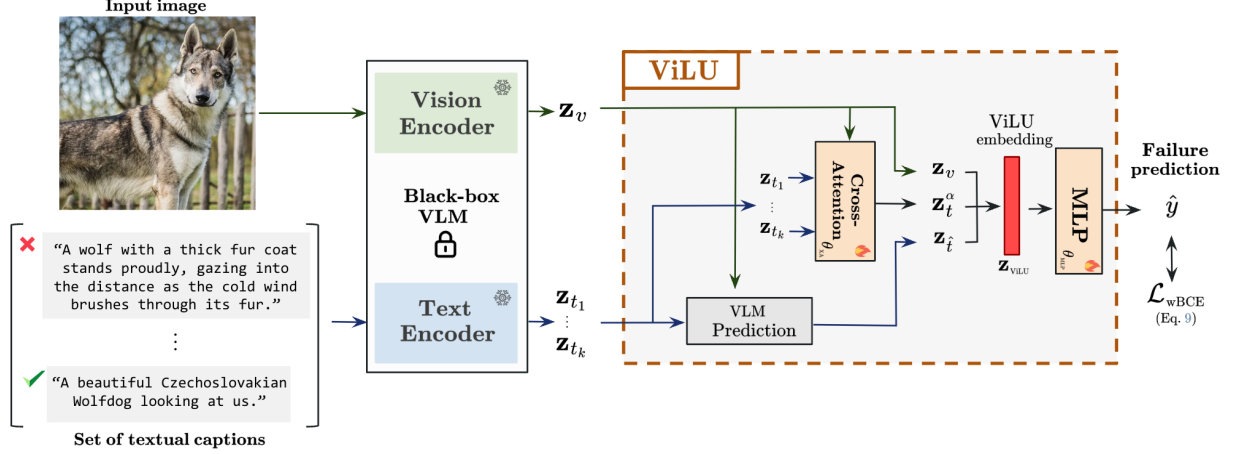


Figure 2. **Overview of ViLU:** A learning-based Vision-Language Uncertainty quantification framework for VLM failure prediction. The key strength of ViLU lies in its ability to contextualize uncertainty estimates by leveraging all textual representations relevant to the task (see Sec. 4.1). It constructs an uncertainty-aware representation by combining the visual embedding z_v , the predicted textual embedding z_i , and an image-conditioned textual representation z_i^α obtained via cross-attention (see Sec. 4.2). Instead of relying on loss prediction, ViLU trains an uncertainty predictor as a binary classifier to distinguish between correct and incorrect predictions (see Sec. 4.3). ViLU is a post-hoc approach that can be efficiently deployed on top of any pre-trained VLM without accessing its weights (black box) and supports both image-caption and image-label tasks.

4.2. ViLU’s architecture

This section details the architectural components of our uncertainty module u_θ and how a visual feature, z_v , for a given sample and textual embeddings of K target concepts, $Z_t = \{z_{t_j}\}_{1 \leq j \leq K}$, are combined to provide an expressive representation for failure detection.

Vision-textual cross-attention. To enable flexible representations of the visual and textual modalities, we employ a *cross-attention module* $h_{\theta_{XA}}$ that produces an image-specific textual representation z_t^α allowing to efficiently capture inherent cross-modal uncertainty:

$$z_t^\alpha = h_{\theta_{XA}}(z_v, z_{t_1}, \dots, z_{t_K}) \quad (4)$$

More specifically, the *query* is the visual representation z_v , and *keys and values* are the K textual embeddings Z_t . The cross-attention’s output is obtained as:

$$\alpha = \text{softmax} \left((W_Q z_v)^\top (W_K Z_t) / \sqrt{d} \right) \quad (5)$$

$$z_t^\alpha = \sum_{j=1}^K \alpha_j (W_V z_{t_j})$$

where α are the attention weights, and W_Q , W_K , and W_V denote the projection matrices for the queries, keys, and values, respectively. This weighted textual embedding refines the textual context based on the model’s predicted distribution over the candidate captions, allowing for a more accurate uncertainty assessment. This contextualized representation can be computed for any number of concepts, ensur-

ing a generic uncertainty module that remains well-defined across different concept sets.

ViLU embeddings. To resolve vision-language ambiguity for failure prediction, our model must capture key information to distinguish correct from incorrect predictions. At a minimum, this requires the visual representation z_v and the textual embedding of the predicted caption z_i , allowing the model to approximate MCM’s uncertainty estimator. However, this limited representation overlooks ambiguous alternatives, making error detection unreliable. To address this, we construct a rich vision-language uncertainty embedding $z_{ViLU} = (z_v, z_i, z_i^\alpha)$ by concatenating z_v , z_i , and the cross-attention output z_i^α .

Learning complex patterns for failure prediction. Detecting misclassifications among numerous fine-grained concepts is challenging, as it requires capturing complex cross-modal relationships. To overcome this, we apply a non-linear transformation on our ViLU embeddings via a multi-layer perceptron (MLP), $g_{\theta_{MLP}}$, which enhances feature expressiveness and produces a scalar uncertainty estimate. Formally, uncertainty quantification is expressed as the predicted failure score \hat{y}_i :

$$\hat{y}_i = \sigma(g_{\theta_{MLP}}(z_{ViLU})), \quad (6)$$

where σ denotes the sigmoid function, ensuring that $\hat{y}_i \rightarrow 1$ when the predicted zero-shot label is likely incorrect. Importantly, $g_{\theta_{MLP}}$ in Eq. (6) boils down to the unnormalized MCM score when using a bilinear form on z_{ViLU} (see Appendix B). Our failure predictor is thus a *consistent generalization of MCM*, incorporating its prior and learning to

refine it for finer multi-modal UQ.

4.3. Training procedure

ViLU accommodates both image-caption and image-label tasks during training and inference.

1) Image-Label Tasks: Image-label classification considers a predefined set of K target categories, leading to a *batch-independent* predictive pipeline. Here, the textual representations of categories are obtained using *text templates* (e.g., "A photo of a [CLASS]"), resulting in a fixed set of textual captions $\{t_j\}_{j \in \{1, \dots, K\}}$. The predicted concept for an image is then determined as:

$$\hat{t}_i = \arg \max_{j \in \{1, \dots, K\}} p(t_j | x_i). \quad (7)$$

This setting is batch-independent, making it suitable for standard classification datasets with predefined labels.

2) Image-Caption Tasks: When a set of textual descriptions is available from an open-vocabulary domain, the goal is to assign the most similar caption to a given input image. It is typically validated using batches of paired images and text descriptions. Given a batch \mathcal{B} of images with associated text descriptions, $\{(x_i, t_i)\}_{i \in \mathcal{B}}$, the predicted concept for an image is determined as:

$$\hat{t}_i = \arg \max_{j \in \mathcal{B}} p(t_j | x_i). \quad (8)$$

Here, the performance is *batch-dependent*, with larger batch sizes increasing task complexity.

Training objective. Our uncertainty module u_θ is trained as a binary classifier to predict VLM zero-shot misclassifications. The parameters $\theta = \{\theta_{\text{XA}}, \theta_{\text{MLP}}\}$ of our uncertainty model are trained by mini-batch gradient descent to minimize the following weighted binary cross-entropy loss:

$$\mathcal{L}_{\text{WBCE}} = -\frac{1}{B} \sum_i [wy_i \log \hat{y}_i + (1 - y_i) \log(1 - \hat{y}_i)] \quad (9)$$

where $y_i = \mathbb{1}_{\{t_i \neq \hat{t}_i\}}$ is the target label, and w is a weighting factor that mitigates the potential class imbalance between correctly and incorrectly classified examples. This weight is dynamically adjusted based on the empirical classification accuracy of the VLM within each mini-batch:

$$w = \log \left(1 + \frac{\sum_{i=1}^B (1 - y_i)}{\sum_{i=1}^B y_i} \right) \quad (10)$$

Previous UQ methods predict the model’s training loss [8, 19, 47], assuming a high loss value indicates misclassification. Applying this approach to VLMs would require predicting CLIP’s [36] contrastive loss or SigLIP’s [50] sigmoid loss, which is impractical in a post-hoc setting where

the pre-training loss is unknown. In contrast, ViLU is loss-agnostic, relying only on whether a prediction is correct. As shown in the experiments Tab. 4, training it as a binary classifier consistently outperforms loss prediction for VLMs, naturally aligning with standard error detection metrics.

5. Experiments

This section presents experimental results validating our multi-modal uncertainty model. We first focus on predicting VLM failures in zero-shot classification across two setups: *i)* standard image-label classification datasets and *ii)* large-scale image-caption datasets. Next, we experimentally analyze the different components of our model and training procedure, conducting various assessments to evaluate its behavior. We provide qualitative results and visualizations illustrating the ability of ViLU to quantify uncertainty.

5.1. Experimental setup

Datasets. We conduct a benchmark across 16 commonly used datasets to evaluate the ability of VLMs to detect misclassification in image classification. As outlined in Sec. 4.3, we consider two settings: *i)* image-label datasets and *ii)* image-caption datasets. Image-label datasets are standard datasets used in CLIP’s transfer learning [22, 52], covering general object recognition, fine-grained classification, and specialized domains (see Appendix A.1). For evaluation, we follow the official data splits provided by each dataset or those proposed in [53]. Image-caption datasets, including CC3M [39], CC12M [4], and LAION-400M [37], contain free-text descriptions for each sample. From these datasets, we randomly hold out 1% of the data for testing.

Implementation details. Unless stated otherwise, we use CLIP ViT-B/32 backbone in all our experiments. Regarding the proposed ViLU, the MLP layer for misclassification prediction follows a four-layer architecture with dimensions [512, 256, 128, 1] and ReLU activations. Training is performed using SGD as the optimizer, with the cross-attention layers remaining frozen during the first epoch. We select the learning rate through a grid search over $\{10^{-1}, 10^{-2}, 10^{-3}\}$ and explore batch sizes among $\{128, 256, 512, 1024\}$.

Baselines. We explore relevant baselines for uncertainty estimation in vision, as well as recent approaches for VLMs. Further details on these baselines and implementation specifics can be found in Appendix A.2. **1) Measures of output distribution:** MCM [30], described in Sec. 3, along with its calibrated variant [15], provide robust uncertainty estimates without additional training. Similarly, Entropy [38] and Doctor [14] are commonly used as baselines for uncertainty estimation. **2) Data-driven predictors:** We implement the recent Rel-U [13], which incorporates cross-label uncertainties in the logit space. However, since Rel-

	CIFAR-10 88.3%		CIFAR-100 68.6%		Caltech101 91.4%		Flowers102 64.0%		OxfordPets 85.1%		Food101 78.9%		ImageNet-1k 62.0%	
	AUC↑	FPR95↓	AUC↑	FPR95↓	AUC↑	FPR95↓	AUC↑	FPR95↓	AUC↑	FPR95↓	AUC↑	FPR95↓	AUC↑	FPR95↓
MCM [30]	89.9	52.1	82.7	67.3	88.1	68.7	86.6	68.0	87.2	59.9	86.4	63.3	80.8	71.3
TS [15] + MCM [30]	89.9	51.5	83.9	68.4	90.4	55.7	86.9	66.0	89.1	<u>55.5</u>	86.9	62.8	80.7	71.5
Entropy [38]	88.7	59.9	79.8	71.9	86.1	78.8	85.5	65.0	88.0	60.0	86.1	65.0	78.3	76.8
Doctor [14]	89.5	56.5	82.3	69.7	88.7	66.5	86.7	63.9	88.9	56.6	86.8	63.4	80.3	72.9
Rel-U [13]	86.2	54.4	81.0	68.2	90.2	58.5	90.0	47.3	83.5	59.3	81.8	73.4	75.1	85.0
LVU [8, 19, 47]	<u>96.6</u>	<u>21.2</u>	80.3	68.5	89.8	50.9	<u>90.5</u>	<u>38.3</u>	84.1	55.7	82.7	69.9	78.7	77.0
BayesVLM [2]	92.6	44.9	<u>87.0</u>	<u>60.3</u>	<u>94.0</u>	<u>37.4</u>	87.3	62.4	<u>89.5</u>	60.3	<u>87.8</u>	<u>60.3</u>	<u>81.5</u>	<u>70.3</u>
ViLU (Ours)	98.3	7.7	91.5	35.4	96.7	18.2	98.7	5.1	94.4	24.5	94.8	28.5	89.5	47.4

	FGVCAircraft 18.1%		EuroSAT 35.8%		StanfordCars 60.1%		DTD 43.0%		SUN397 62.1%		UCF101 61.6%		Average 62.7%	
	AUC↑	FPR95↓	AUC↑	FPR95↓	AUC↑	FPR95↓	AUC↑	FPR95↓	AUC↑	FPR95↓	AUC↑	FPR95↓	AUC↑	FPR95↓
MCM [30]	<u>75.7</u>	82.9	64.1	87.6	81.4	73.4	77.4	77.9	78.8	75.9	84.1	68.9	81.8	70.6
TS [15] + MCM [30]	74.9	82.9	63.0	88.1	81.6	71.9	76.9	78.3	79.0	75.5	84.5	69.7	82.0	69.5
Entropy [38]	74.1	83.6	61.0	92.1	79.4	77.5	76.4	80.2	75.8	78.6	83.5	72.9	80.2	74.0
Doctor [14]	74.8	82.9	62.4	89.5	80.9	73.1	76.9	82.6	78.2	77.2	84.5	70.2	81.6	71.2
Rel-U [13]	68.6	<u>82.5</u>	76.3	72.1	75.5	78.9	81.4	69.7	75.2	81.3	84.1	61.1	80.7	68.6
LVU [8, 19, 47]	74.8	<u>83.5</u>	<u>95.9</u>	<u>19.3</u>	78.4	75.4	<u>87.2</u>	<u>55.9</u>	76.7	76.9	<u>88.6</u>	<u>53.6</u>	<u>85.0</u>	<u>57.4</u>
BayesVLM [2]	70.9	84.3	74.3	86.6	<u>87.7</u>	<u>63.4</u>	77.6	77.0	<u>80.3</u>	<u>73.4</u>	84.6	66.2	84.2	65.1
ViLU (Ours)	81.0	71.7	98.8	4.4	90.1	46.8	93.8	28.8	88.6	50.3	95.9	20.9	93.2	29.9

Table 1. **Misclassification detection on image-label datasets.** The evaluation leverages each dataset’s labeled classes as textual queries, which are fixed for each batch. Values below dataset names denote CLIP zero-shot accuracy on the respective dataset.

U relies on label-based information, it does not apply to image-caption datasets. Additionally, we assess methods that leverage embedding representations to learn patterns related to uncertainty. Specifically, we compare against baselines that predict classifier loss, such as ConfidNet [8] and other vision-only estimators [19, 47], collectively referred to as ‘Learning Visual Uncertainty’ (LVU). Finally, we evaluate the most recent post-hoc UQ probabilistic modeling approach designed for VLMs, BayesVLM [2].

Metrics. To assess the performance of our uncertainty model, we rely on two standard metrics: **1)** False Positive Rate at 95% True Positive Rate (**FPR95**) and **2)** Area Under the receiver-operating characteristic Curve (**AUC**). These are commonly used in failure prediction to quantify the model’s ability to detect incorrect classifications [8, 13, 14].

5.2. Main results

Image classification datasets. In Tab. 1, we evaluate misclassification detection on CLIP’s zero-shot predictions across 13 standard image-label datasets. Notably, MCM emerges as a strong baseline in this setting, even outperforming more complex methods such as Doctor and Rel-U. This advantage arises because these methods rely on task-specific vision classifiers, which are generally less well-calibrated than large-scale pre-trained models. Consequently, MCM achieves superior performance without requiring post-processing steps, such as temperature scaling [15], for failure prediction. On the other hand, expressive data-driven methods such as LVU, BayesVLM,

and our proposed ViLU enable more effective failure detection. Our proposed ViLU ranks first across all datasets and metrics. Its novel architectural design leverages the class-semantic information embedded in MCM while also capturing uncertainty patterns specific to each sample’s ambiguities. As a clear demonstration of its effectiveness, ViLU achieves remarkable improvements in FPR95, surpassing MCM, BayesVLM, and LVU by margins of -40.7 , -35.2 , and -27.5 , respectively (Tab. 1, Average column).

CLIP’s zero-shot accuracy for each dataset is reported in Tab. 1. MCM and BayesVLM performances closely follow CLIP’s accuracy, struggling in low zero-shot accuracy settings: they achieve only 64.1% and 74.3% AUC in EuroSAT, a dataset on which CLIP’s accuracy is 35.8%. This limitation makes them unreliable when zero-shot accuracy is low – an unpredictable scenario in real-world settings. In contrast, ViLU remains effective across all accuracy regimes. See Appendix C for further analysis.

Large-scale image-caption datasets. We now evaluate the ability of state-of-the-art methods to detect failures in open-vocabulary settings, where tasks vary based on the inference batch and its specific captions. Tab. 2 presents results for applicable baselines in this challenging setting, along with the proposed ViLU. Unlike in previous experiments on image-label datasets, LVU fails to outperform even the MCM baseline, underscoring the importance of considering target objectives alongside sample-related uncertainties in open-vocabulary scenarios. As a result, methods specifically designed for vision-language models,

	CC3M 58.8%		CC12M 73.5%		LAION-400M 90.5%	
	AUC↑	FPR95↓	AUC↑	FPR95↓	AUC↑	FPR95↓
MCM [30]	83.9	69.0	88.8	58.8	91.7	50.2
Entropy [38]	82.5	73.3	87.7	63.0	89.4	62.5
Doctor [14]	83.7	70.1	88.6	59.9	91.2	54.5
LVU [8, 19, 47]	69.3	82.5	74.4	76.5	80.2	72.3
BayesVLM [2]	87.1	62.6	90.9	53.3	95.1	26.4
ViLU (Ours)	91.4	41.1	95.2	25.2	97.3	21.2

Table 2. **Misclassification detection on image-caption datasets.** The evaluation uses the captions of each randomly-retrieved batch as textual queries. Hence, the textual queries vary for each batch. Results reported with a batch size of 1024 samples for inference.

such as BayesVLM, achieve superior performance across all three evaluated datasets. Our proposed ViLU achieves the best performance, consistently surpassing BayesVLM with FPR95 improvements of -21.5 , -28.1 , and -5.2 on CC3M, CC12M, and LAION-400M, respectively. This advantage stems from our explicit modeling of misclassification errors, whereas BayesVLM focuses on the uncertainty of similarities between individual embeddings, which is more implicit.

5.3. Ablation studies

Architectural design of ViLU. Tab. 3 highlights the contributions of different components in our model, namely the cross-attention mechanism and the inclusion of the predicted caption as input. As observed in [8, 19], using **only visual information** (first row) is effective on CIFAR-10 but struggles on larger datasets with fine-grained or semantically similar concepts. For instance, on ImageNet-1k, visual information alone fails to outperform MCM. Incorporating the **predicted class textual embedding** (second row) significantly improves performance across all datasets, yielding a +10 AUC gain on ImageNet-1k and +14 AUC on CC12M. This additional input helps the model to handle class ambiguity, which is crucial for datasets where categories are easily confused. For example, as shown in Fig. 3, the class `container ship` is often misclassified as `ocean liner`, another type of boat. Finally, the **cross-attention module** (third row) enables the model to integrate contextual information from all candidate classes or captions. By re-contextualizing predictions among available textual inputs, this mechanism proves particularly beneficial for CC12M, where captions change dynamically across batches. Unlike CIFAR-10 and ImageNet-1k, where class sets are fixed, omitting cross-attention in CC12M results in an AUC plateau at 88.9, only slightly above MCM. Incorporating this mechanism enhances the model’s ability to detect ambiguities and assess potential errors.

Loss function design for failure prediction. In Sec. 4.3, we discussed our optimization target and choice of loss

Visual embed.	Cross attention	Predicted caption	CIFAR-10		ImageNet-1k		CC12M	
			AUC↑	FPR95↓	AUC↑	FPR95↓	AUC↑	FPR95↓
✓	✗	✗	96.4	21.8	78.7	77.0	74.0	76.5
✓	✗	✓	97.9	10.8	88.8	50.1	88.9	48.9
✓	✓	✗	97.7	11.4	86.1	63.5	93.6	37.0
✓	✓	✓	98.3	8.2	89.5	47.4	95.2	25.2
MCM [30]			89.9	52.1	80.8	71.3	88.8	58.8

Table 3. **Ablation on different components of ViLU.**

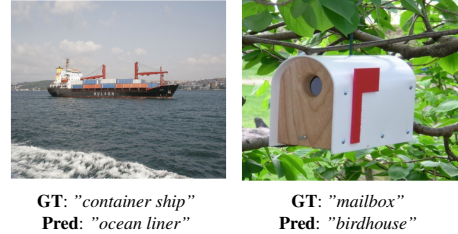


Figure 3. **Two qualitative examples.** Misclassifications detected by ViLU, but not MCM [30] and visual-only baselines [8, 19].

function. Unlike prior works [8, 19, 47], which treat the problem as a regression task by directly predicting the test-time loss and optimizing it with MSE, we instead frame it as a binary classification task, distinguishing between errors and correct predictions. As shown in Tab. 4, this approach consistently outperforms MSE-based loss approximations, yielding a +3 AUC improvement on ImageNet-1k while reducing FPR95 by 16 points. Additionally, our automatic weighting of the two classes (misclassified and correctly classified) further enhances the performance, resulting in a +1 AUC gain on ImageNet-1k and a 2-point reduction in FPR95 on CIFAR-10.

	CIFAR-10		ImageNet-1k	
	AUC↑	FPR95↓	AUC↑	FPR95↓
MSE [8, 19]	95.1	30.4	84.8	64.4
w/ Weighting	95.6	29.6	85.7	63.2
BCE	97.7	10.5	88.6	48.4
w/ Weighting (Ours)	98.3	8.2	89.5	47.4

Table 4. **Role of the proposed weighted loss.** Effect of loss function choice and adaptive weighting in Eq. (10) for failure detection.

5.4. In-depth analysis

Classification complexity on image-caption datasets. Fig. 4 explores the performance of ViLU in challenging image-caption classification tasks, where difficulty is determined by the number of concepts to be distinguished simultaneously, *i.e.*, batch size used for inference. Naturally, increasing the batch size makes the classification more complex, making errors harder to detect for methods that rely on semantic relationships among query concepts, such as ViLU or MCM. However, ViLU consistently outperforms

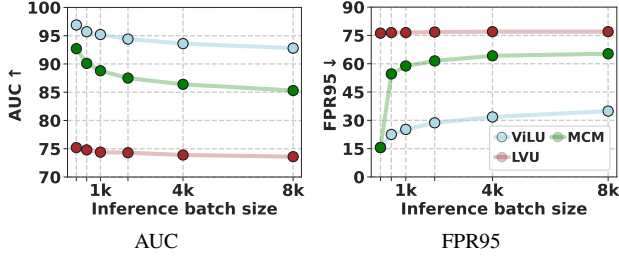


Figure 4. **Robustness to image-caption task complexity.** Inference batch size effect in failure detection for ViLU (CC12M).

MCM across all batch sizes. Notably, this configuration does not affect prior LVU methods, which estimate vision-only uncertainty. However, they fall short in performance, particularly compared to the proposed ViLU.

Requirements on training data. As a data-driven uncertainty quantifier, the proposed ViLU requires a subset of image-caption or image-label examples. Fig. 5 illustrates the data-efficiency of the proposed approach for uncertainty quantification. The results showcase the efficiency of ViLU, which *requires only a small amount of data to surpass the strong baseline MCM*, e.g., 2.5% for ImageNet and even less for specialized datasets such as EuroSAT.

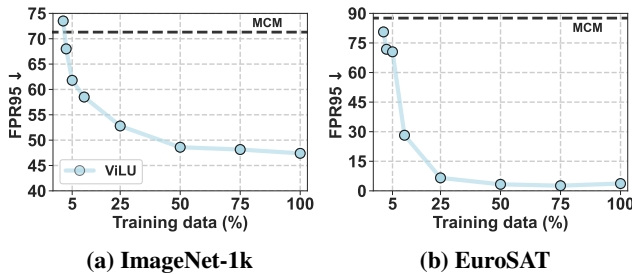


Figure 5. **Data-efficiency.** Performance, in terms of FPR95 \downarrow , w.r.t. the available data for training ViLU.

Cross-datasets generalization. To evaluate cross-task generalization without per-dataset training and show ViLU’s robustness to dataset shifts, we report in Tab. 5 transfer results of ViLU pre-trained on the large-scale CCM12 dataset, showing that *it generalizes well on the 12 datasets* in Tab. 5, outperforming MCM in this pure transfer setting. Tab. 5 also showcases the clear superiority of ViLU over LVU (trained on CC12M), underscoring the critical importance of modeling vision-language uncertainty for zero-shot generalization. This suggests significant room for improving ViLU pre-training, as the lightweight model is not specifically designed for this task. Non-trivial directions include backbone fine-tuning, advanced data augmentation, and smarter batch sampling.

Dataset	MCM	LVU	ViLU
CIFAR-10	52.1	77.2	54.2
CIFAR-100	67.3	83.8	59.9
Caltech101	68.7	82.5	48.8
Flowers102	68.0	96.8	67.4
OxfordPets	59.9	93.1	58.1
Food101	63.3	87.2	67.4
FGVCAircraft	82.9	94.5	82.3
EuroSAT	87.6	88.2	85.7
DTD	77.9	93.1	78.2
SUN397	75.9	90.1	72.7
StanfordCars	73.4	92.6	84.1
UCF101	68.9	90.4	63.8
Average	70.5	89.1	68.6

Table 5. FPR95 \downarrow across datasets. Zero-shot performance when pre-trained on CC12M.

Extension to different VLMs. Tab. 6 shows the performance of ViLU on various zero-shot vision-language backbones, including CLIP [36] and SigLIP [50]. ViLU consistently outperforms MCM across different CLIP/SigLIP models (e.g., ViT-B/16, ViT-L/14). Unlike LVU methods [8, 19, 47], ViLU operates without access to the VLM’s pre-training loss, relying only on classification correctness, ensuring broad applicability across different VLMs.

	Backbone	Method	CIFAR-10		ImageNet-1k	
			AUC \uparrow	FPR95 \downarrow	AUC \uparrow	FPR95 \downarrow
CLIP [36]	ViT-B/16	MCM [30]	90.9	47.3	81.0	73.0
		ViLU	98.4	8.0	90.3	44.2
	ViT-L/14	MCM [30]	93.6	31.5	82.9	68.9
		ViLU	99.0	4.1	91.2	39.2
SigLIP [50]	ViT-B/16	MCM [30]	92.8	46.1	84.2	65.8
		ViLU	97.6	13.3	90.7	44.4
	ViT-L/16	MCM [30]	95.6	29.1	86.8	64.1
		ViLU	98.4	7.8	91.3	41.4

Table 6. **Generalization across backbones.** ViLU shows consistent performance gains on several VLMs compared to MCM.

Qualitative assessment. In Fig. 3, we present two qualitative examples from ImageNet where the VLM misclassified the input images. On the left, the model predicted `ocean liner` instead of `container ship`, likely due to their shared visual features as large vessels. On the right, a mailbox was misclassified as a birdhouse, possibly influenced by the surrounding vegetation and the mailbox’s opening, which resemble typical birdhouse features. ViLU effectively captures both sources of ambiguity: semantic confusion between visually similar classes and misinterpretations driven by contextual cues.

Uncertainty distribution score. Fig. 6 illustrates the effectiveness of different uncertainty estimation methods in distinguishing between correctly and incorrectly classified samples on ImageNet. In MCM and LVU, the uncertainty distributions for success and failure overlap significantly.

In contrast, ViLU produces a more distinct separation. Indeed, misclassified samples receive high uncertainty (peaking near 1.0), while correct predictions have low uncertainty (peaking near 0.0). Its higher density at the extremes indicates a well-calibrated uncertainty measure.

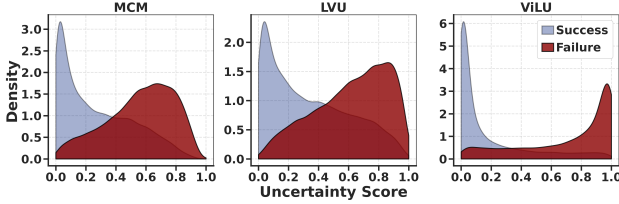


Figure 6. **Uncertainty score distribution.** Predictions for correctly and incorrectly classified samples on ImageNet.

6. Conclusion

We have presented our ViLU method, a new uncertainty quantification approach for failure prediction of pre-trained VLMs. ViLU learns an appropriate uncertainty embedding space including fine interactions between visual and concepts ambiguities to learn an effective binary failure predictor on the downstream task. Extensive experiments on several datasets show the significant gain of our method compared to state-of-the-art UQ methods for failure prediction. In addition, ablation studies clearly validate our architectural choices and training design. We also show that ViLU remains effective even in the low-performance regime of VLMs, in contrast to MCM [30] or BayesVLM [2]. Future works include adjusting ViLU in the context of domain adaptation and test-time adaptation of VLMs.

References

- [1] Max Bain, Arsha Nagrani, Gül Varol, and Andrew Zisserman. A CLIP-hitchhiker’s guide to long video retrieval. *arXiv preprint arXiv:2205.08508*, 2022. 2
- [2] Anton Baumann, Rui Li, Marcus Klasson, Santeri Mentu, Shyamgopal Karthik, Zeynep Akata, Arno Solin, and Martin Trapp. Post-hoc probabilistic vision-language models. *arXiv preprint arXiv:2412.06014*, 2024. 1, 2, 3, 6, 7, 9, 13
- [3] Lukas Bossard, Matthieu Guillaumin, and Luc Van Gool. Food-101 – mining discriminative components with random forests. In *European Conference on Computer Vision (ECCV)*, 2014. 12
- [4] Soravit Changpinyo, Piyush Sharma, Nan Ding, and Radu Soricut. Conceptual 12m: Pushing web-scale image-text pre-training to recognize long-tail visual concepts. In *IEEE Conference on Computer Vision and Pattern Recognition, CVPR 2021, virtual, June 19-25, 2021*, pages 3558–3568. Computer Vision Foundation / IEEE, 2021. 5
- [5] Sanghyuk Chun. Improved probabilistic image-text representations. In *The Twelfth International Conference on Learning Representations*, 2024. 3
- [6] Sanghyuk Chun, Seong Joon Oh, Rafael Sampaio De Rezende, Yannis Kalantidis, and Diane Larlus. Probabilistic embeddings for cross-modal retrieval. In *Proceedings of the IEEE/CVF Conference on Computer Vision and Pattern Recognition (CVPR)*, pages 8415–8424, 2021. 3
- [7] Mircea Cimpoi, Subhransu Maji, Iasonas Kokkinos, Sammy Mohamed, and Andrea Vedaldi. Describing textures in the wild. In *Proceedings of the IEEE/CVF Conference on Computer Vision and Pattern Recognition (CVPR)*, pages 3606–3613, 2014. 12
- [8] Charles Corbière, Nicolas Thome, Avner Bar-Hen, Matthieu Cord, and Patrick Pérez. Addressing failure prediction by learning model confidence. *Advances in Neural Information Processing Systems*, 32, 2019. 1, 2, 5, 6, 7, 8, 12, 13, 14
- [9] Matt Deitke, Christopher Clark, Sangho Lee, Rohun Tripathi, Yue Yang, Jae Sung Park, Mohammadreza Salehi, Niklas Muennighoff, Kyle Lo, Luca Soldaini, et al. Molmo and pixmo: Open weights and open data for state-of-the-art multimodal models. *arXiv preprint arXiv:2409.17146*, 2024. 1, 2
- [10] Jia Deng, Wei Dong, Richard Socher, Li-Jia Li, Kai Li, and Li Fei-Fei. Imagenet: A large-scale hierarchical image database. In *Proceedings of the IEEE/CVF Conference on Computer Vision and Pattern Recognition (CVPR)*, pages 248–255, 2009. 12
- [11] Li Fei-Fei, R. Fergus, and P. Perona. Learning generative visual models from few training examples: An incremental bayesian approach tested on 101 object categories. In *Proceedings of the IEEE/CVF Conference on Computer Vision and Pattern Recognition Workshops (CVPRW)*, pages 178–178, 2004. 12
- [12] Yarin Gal and Zoubin Ghahramani. Dropout as a bayesian approximation: representing model uncertainty in deep learning. In *Proceedings of the 33rd International Conference on International Conference on Machine Learning - Volume 48*, page 1050–1059. JMLR.org, 2016. 1
- [13] Eduardo Dadoalto Câmara Gomes, Marco Romanelli, Georg Pichler, and Pablo Piantanida. A data-driven measure of relative uncertainty for misclassification detection. In *The Twelfth International Conference on Learning Representations*, 2024. 2, 5, 6, 12
- [14] Federica Granese, Marco Romanelli, Daniele Gorla, Catuscia Palamidessi, and Pablo Piantanida. Doctor: A simple method for detecting misclassification errors. *Advances in Neural Information Processing Systems*, 34:5669–5681, 2021. 2, 5, 6, 7, 12
- [15] Chuan Guo, Geoff Pleiss, Yu Sun, and Kilian Q. Weinberger. On calibration of modern neural networks. In *International Conference on Machine Learning (ICML)*, pages 1321–1330, 2017. 5, 6, 12
- [16] Patrick Helber, Benjamin Bischke, Andreas Dengel, and Damian Borth. Introducing eurosat: A novel dataset and deep learning benchmark for land use and land cover classification. In *IEEE International Geoscience and Remote Sensing Symposium (IGARSS)*, pages 3606–3613, 2018. 12
- [17] Dan Hendrycks and Kevin Gimpel. A baseline for detecting misclassified and out-of-distribution examples in neural net-

- works. In *The Fifth International Conference on Learning Representations*. OpenReview.net, 2017. 1, 2
- [18] Siteng Huang, Biao Gong, Yulin Pan, Jianwen Jiang, Yiliang Lv, Yuyuan Li, and Donglin Wang. Vop: Text-video co-operative prompt tuning for cross-modal retrieval. In *Proceedings of the IEEE/CVF conference on computer vision and pattern recognition (CVPR)*, pages 6565–6574, 2023. 2
- [19] Michael Kirchhof, Mark Collier, Seong Joon Oh, and Enkelejda Kasneci. Pretrained visual uncertainties. *arXiv preprint arXiv:2402.16569*, 2024. 1, 2, 5, 6, 7, 8, 12, 13
- [20] Jonathan Krause, Michael Stark, Jia Deng, and Li Fei-Fei. 3d object representations for fine-grained categorization. In *Proceedings of the IEEE/CVF Conference on Computer Vision and Pattern Recognition (CVPR)*, page 3498–3505, 2012. 12
- [21] Alex Krizhevsky, Geoffrey Hinton, et al. Learning multiple layers of features from tiny images.(2009), 2009. 12
- [22] Marc Lafon, Elias Ramzi, Clément Rambour, Nicolas Audebert, and Nicolas Thome. Gallop: Learning global and local prompts for vision-language models. In *European Conference on Computer Vision*, pages 264–282. Springer, 2024. 2, 5
- [23] Mengcheng Lan, Chaofeng Chen, Yiping Ke, Xinjiang Wang, Litong Feng, and Wayne Zhang. Proxyclip: Proxy attention improves clip for open-vocabulary segmentation. In *European Conference on Computer Vision*, pages 70–88. Springer, 2024. 2
- [24] Hugo Laurençon, Lucile Saulnier, Léo Tronchon, Stas Bekman, Amanpreet Singh, Anton Lozhkov, Thomas Wang, Siddharth Karamcheti, Alexander Rush, Douwe Kiela, et al. Obelics: An open web-scale filtered dataset of interleaved image-text documents. *Advances in Neural Information Processing Systems*, 36, 2024. 2
- [25] Hugo Laurençon, Leo Tronchon, Matthieu Cord, and Victor Sanh. What matters when building vision-language models? In *The Thirty-eighth Annual Conference on Neural Information Processing Systems*, 2024. 1, 2
- [26] Hao Li, Jingkuan Song, Lianli Gao, Pengpeng Zeng, Haonan Zhang, and Gongfu Li. A differentiable semantic metric approximation in probabilistic embedding for cross-modal retrieval. In *Advances in Neural Information Processing Systems*, 2022. 3
- [27] Junnan Li, Dongxu Li, Silvio Savarese, and Steven Hoi. Blip-2: Bootstrapping language-image pre-training with frozen image encoders and large language models. In *International conference on machine learning*, pages 19730–19742. PMLR, 2023. 1, 2
- [28] S. Maji, J. Kannala, E. Rahtu, M. Blaschko, and A. Vedaldi. Fine-grained visual classification of aircraft. In *ArXiv Preprint*, 2013. 12
- [29] Matthias Minderer, Josip Djolonga, Rob Romijnders, Frances Hubis, Xiaohua Zhai, Neil Houlsby, Dustin Tran, and Mario Lucic. Revisiting the calibration of modern neural networks. *Advances in neural information processing systems*, 34:15682–15694, 2021. 3
- [30] Yifei Ming, Ziyang Cai, Jiuxiang Gu, Yiyu Sun, Wei Li, and Yixuan Li. Delving into out-of-distribution detection with vision-language representations. *Advances in neural information processing systems*, 35:35087–35102, 2022. 1, 2, 3, 5, 6, 7, 8, 9, 12, 13
- [31] Balamurali Murugesan, Julio Silva-Rodríguez, Ismail Ben Ayed, and Jose Dolz. Robust calibration of large vision-language adapters. In *European Conference on Computer Vision*, pages 147–165, 2024. 1
- [32] Andrei Neculai, Yanbei Chen, and Zeynep Akata. Probabilistic compositional embeddings for multimodal image retrieval. *Proceedings of the IEEE/CVF Conference on Computer Vision and Pattern Recognition Workshops (CVPRW)*, pages 4546–4556, 2022. 3
- [33] Maria-Elena Nilsback and Andrew Zisserman. Automated flower classification over a large number of classes. In *Indian Conference on Computer Vision, Graphics and Image Processing*, 2008. 12
- [34] Changdae Oh, Hyesu Lim, Mijoo Kim, Dongyoon Han, Sangdoo Yun, Jaegul Choo, Alexander Hauptmann, Zhi-Qi Cheng, and Kyungwoo Song. Towards calibrated robust fine-tuning of vision-language models. *Advances in Neural Information Processing Systems*, 37:12677–12707, 2024. 1
- [35] Omkar M Parkhi, Andrea Vedaldi, Andrew Zisserman, and CV Jawahar. Cats and dogs. In *Proceedings of the IEEE/CVF Conference on Computer Vision and Pattern Recognition (CVPR)*, page 3498–3505, 2012. 12
- [36] Alec Radford, Jong Wook Kim, Chris Hallacy, Aditya Ramesh, Gabriel Goh, Sandhini Agarwal, Girish Sastry, Amanda Askell, Pamela Mishkin, Jack Clark, et al. Learning transferable visual models from natural language supervision. In *International conference on machine learning*, pages 8748–8763. PMLR, 2021. 1, 2, 5, 8
- [37] Christoph Schuhmann, Richard Vencu, Romain Beaumont, Robert Kaczmarczyk, Clayton Mullis, Aarush Katta, Theo Coombes, Jenia Jitsev, and Aran Komatsuzaki. LAION-400M: open dataset of clip-filtered 400 million image-text pairs. *CoRR*, abs/2111.02114, 2021. 1, 2, 5
- [38] Murat Sensoy, Lance M. Kaplan, and Melih Kandemir. Evidential deep learning to quantify classification uncertainty. In *Advances in Neural Information Processing Systems 31: Annual Conference on Neural Information Processing Systems 2018, NeurIPS 2018, December 3-8, 2018, Montréal, Canada*, pages 3183–3193, 2018. 2, 5, 6, 7, 12
- [39] Piyush Sharma, Nan Ding, Sebastian Goodman, and Radu Soricut. Conceptual captions: A cleaned, hypemymed, image alt-text dataset for automatic image captioning. In *Proceedings of the 56th Annual Meeting of the Association for Computational Linguistics, ACL 2018, Melbourne, Australia, July 15-20, 2018, Volume 1: Long Papers*, pages 2556–2565. Association for Computational Linguistics, 2018. 5
- [40] Khurram Soomro, Amir Roshan Zamir, and Mubarak Shah. Ucf101: A dataset of 101 human actions classes from videos in the wild. In *ArXiv Preprint*, 2012. 12
- [41] Weijie Tu, Weijian Deng, and Tom Gedeon. A closer look at the robustness of contrastive language-image pre-training (clip). *Advances in Neural Information Processing Systems*, 36:13678–13691, 2023. 3

- [42] Uddeshya Upadhyay, Shyamgopal Karthik, Massimiliano Mancini, and Zeynep Akata. Probylm: Probabilistic adapter for frozen vision-language models. In *Proceedings of the IEEE/CVF International Conference on Computer Vision*, pages 1899–1910, 2023. [1](#), [2](#), [3](#), [12](#)
- [43] Feng Wang, Jieru Mei, and Alan Yuille. Sclip: Rethinking self-attention for dense vision-language inference. In *European Conference on Computer Vision*, pages 315–332. Springer, 2024. [2](#)
- [44] Shuoyuan Wang, Jindong Wang, Guoqing Wang, Bob Zhang, Kaiyang Zhou, and Hongxin Wei. Open-vocabulary calibration for fine-tuned CLIP. In *Proceedings of the 41st International Conference on Machine Learning*, pages 51734–51754, 2024. [1](#)
- [45] Jianxiong Xiao, James Hays, Krista A. Ehinger, Aude Oliva, and Antonio Torralba. Sun database: Large-scale scene recognition from abbey to zoo. In *Proceedings of the IEEE/CVF Conference on Computer Vision and Pattern Recognition (CVPR)*, pages 3485–3492, 2010. [12](#)
- [46] Jingkan Yang, Kaiyang Zhou, Yixuan Li, and Ziwei Liu. Generalized out-of-distribution detection: A survey, 2024. [1](#)
- [47] Donggeun Yoo and In So Kweon. Learning loss for active learning. In *Proceedings of the IEEE/CVF Conference on Computer Vision and Pattern Recognition (CVPR)*, pages 93–102, 2019. [1](#), [2](#), [5](#), [6](#), [7](#), [8](#), [12](#), [13](#)
- [48] Hee Suk Yoon, Eunseop Yoon, Joshua Tian Jin Tee, Mark A Hasegawa-Johnson, Yingzhen Li, and Chang D Yoo. C-TPT: Calibrated test-time prompt tuning for vision-language models via text feature dispersion. In *The Twelfth International Conference on Learning Representations*, 2024. [1](#)
- [49] Qihang Yu, Ju He, Xueqing Deng, Xiaohui Shen, and Liang-Chieh Chen. Convolutions die hard: Open-vocabulary segmentation with single frozen convolutional clip. *Advances in Neural Information Processing Systems*, 36:32215–32234, 2023. [2](#)
- [50] Xiaohua Zhai, Basil Mustafa, Alexander Kolesnikov, and Lucas Beyer. Sigmoid loss for language image pre-training. In *Proceedings of the IEEE/CVF International Conference on Computer Vision*, pages 11975–11986, 2023. [1](#), [2](#), [5](#), [8](#)
- [51] Zhuowen Tu Zheng Ding, Jieke Wang. Open-vocabulary universal image segmentation with maskclip. In *International Conference on Machine Learning*, 2023. [2](#)
- [52] Kaiyang Zhou, Jingkan Yang, Chen Change Loy, and Ziwei Liu. Conditional prompt learning for vision-language models. In *Proceedings of the IEEE/CVF conference on computer vision and pattern recognition (CVPR)*, pages 16816–16825, 2022. [2](#), [5](#)
- [53] Kaiyang Zhou, Jingkan Yang, Chen Change Loy, and Ziwei Liu. Learning to prompt for vision-language models. *International Journal of Computer Vision*, 130(9):2337–2348, 2022. [5](#)
- [54] Kaiyang Zhou, Jingkan Yang, Chen Change Loy, and Ziwei Liu. Learning to prompt for vision-language models. *International Journal of Computer Vision*, 130(9):2337–2348, 2022. [2](#)

ViLU: Learning Vision-Language Uncertainties for Failure Prediction

Supplementary Material

A. Additional details on experimental setup

A.1. Datasets

In this section, we provide additional details on the image-label datasets used in the main experiments presented in the paper. These span general object recognition, fine-grained classification, and specialized domains. The datasets include ImageNet-1k [10], CIFAR-10 [21], CIFAR-100 [21], SUN397 [45], FGVC Aircraft [28], EuroSAT [16], StanfordCars [20], Food101 [3], OxfordPets [35], Flowers102 [33], Caltech101 [11], DTD [7], and UCF101 [40].

A.2. Baselines & Implementation

- **MCM [30]:** Maximum Concept Matching (MCM) estimates uncertainty in VLMs by leveraging the softmax probability distribution over all classes or captions. It selects the most likely caption for an image based on the highest probability score, providing a natural measure of confidence in the model’s predictions. No additional training is required since MCM directly uses the model’s output probabilities.
- **MCM + TS [15]:** This method extends MCM by applying Temperature Scaling (TS) to adjust the softmax probabilities better. TS optimizes the temperature parameter to refine the confidence scores, leading to more calibrated uncertainty estimates. The multiplicative temperature parameter is learned using the whole training dataset to minimize expected calibration error, using LBFGS optimizer.
- **Entropy [38]:** This method quantifies uncertainty in neural network predictions by calculating the Shannon entropy of the output probability distribution. High entropy indicates more significant uncertainty, as the model assigns similar probabilities across multiple classes, reflecting ambiguity in its prediction. On the other hand, low entropy signifies confidence, with the model favoring a specific class. Entropy-based uncertainty estimation does not require additional training.
- **DOCTOR [14]:** DOCTOR quantifies uncertainty by analyzing the confidence distribution of the model’s predictions. It computes the Rényi entropy of order two, a measure based on the squared probabilities assigned to each class, emphasizing how concentrated or dispersed the probability mass is. A prediction with one dominant probability value will yield a low uncertainty score, while a more evenly spread distribution results in higher uncertainty. This method does not require additional training and operates directly on the model’s softmax outputs.
- **Rel-U [13]:** Rel-U is a data-driven method that in-

corporates cross-label uncertainties directly in the logit space. Learning relationships between class logits provides a refined estimation of uncertainty beyond traditional confidence scores. Due to its reliance on a cross-label cost penalty matrix, Rel-U does not apply to image-text datasets where labels are absent. Rel-U’s hyperparameters are fixed to $\lambda = 0.15$ and $T = 0.5$ greedily, since they provided the best performance.

- **Learning Visual Uncertainties (LVU) [8, 19, 47]:** LVU refers to a class of models designed to predict the loss of a visual backbone as a means to estimate potential errors. ConfidNet [8] established that accurately predicting uncertainty is equivalent to estimating the model’s loss—if a model can predict the loss of its visual backbone, it inherently quantifies its error. Another approach, Pretrained Visual Uncertainties [19], follows a similar principle by learning to predict backbone loss, leveraging pretraining on ImageNet-21k.

Implementation: To evaluate the LVU baseline, we use the same MLP architecture as our model but restrict the input to the visual token only. Additionally, following [8, 19], this baseline is trained with an MSE loss, in contrast to our method, which uses a BCE loss.

- **ProbVLM [42]:** ProbVLM introduces a probabilistic adapter that estimates probability distributions for embeddings of pre-trained VLMs. This is achieved through inter- and intra-modal alignment in a post-hoc manner. The goal is to capture the inherent ambiguity in embeddings, reflecting the fact that multiple samples can represent the same concept in the physical world. This method enhances the calibration of embedding uncertainties in retrieval tasks and benefits downstream applications like active learning and model selection.

Implementation: ProbVLM models probability distributions over the embeddings of image and text modalities. However, it does not explicitly model the uncertainty in their interaction via cosine similarity. As a result, directly adapting the method for image classification is not straightforward. We attempted to include ProbVLM in our baseline comparison by using its proposed visual aleatoric uncertainty metric, but it resulted in nearly random failure prediction performance. Additionally, we explored using its cross-modal loss as an uncertainty logit, applying a softmax transformation, but this approach also proved ineffective. In contrast, BayesVLM addresses this limitation by modeling the uncertainty over the similarity computation, enabling a more principled approach to downstream tasks like image classification.

- **BayesVLM [2]:** BayesVLM is a training-free method for estimating predictive uncertainty. It employs a post-hoc approximation of the Bayesian posterior, allowing for analytic computation of uncertainty propagation through the VLM. By approximating the Bayesian posterior over model parameters, BayesVLM captures uncertainties inherent to the model itself (image and text encoders). These model uncertainties are then propagated through the VLM to produce uncertainty estimates for predictions. **Implementation:** To evaluate BayesVLM, we follow the implementation provided in its official Github repository <https://github.com/AaltoML/BayesVLM>

B. Additional details on ViLU

In Sec. 4.2 of the main paper, we mentioned that ViLU is a consistent generalization of MCM. More precisely, the uncertainty module g_θ can model the unnormalized MCM score by approximating the following bilinear form on $\mathbf{z}_{\text{ViLU}} = (\mathbf{z}_v, \mathbf{z}_{\hat{t}}, \mathbf{z}_t^\alpha)$:

$$g_\theta(\mathbf{z}_{\text{ViLU}}) = \frac{1}{2} \mathbf{z}_{\text{ViLU}}^T A \mathbf{z}_{\text{ViLU}} = \mathbf{z}_v^T \mathbf{z}_{\hat{t}}, \quad (11)$$

$$\text{with } A = \begin{pmatrix} 0 & I_d & 0 \\ I_d & 0 & 0 \\ 0 & 0 & 0 \end{pmatrix} \in \mathbb{R}^{3d \times 3d}.$$

C. Additional experimental results

C.1. Impact of MLP depth on performance

The results in Fig. 7 show that ViLU is relatively robust to MLP depth variations, particularly on ImageNet, where performance remains stable across different configurations. Across all tested datasets, a depth of 4 layers consistently achieved strong results, suggesting that this architecture provides a good balance between expressiveness and generalization for failure prediction.

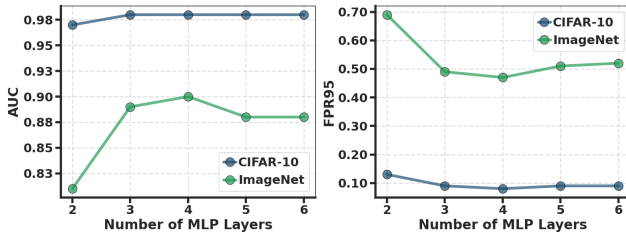


Figure 7. **Impact of MLP depth.** Performance of ViLU on ImageNet and CIFAR-10 for different MLP depths.

C.2. Robustness to image-text task complexity

Tab. 7 provides the quantitative results corresponding to the uncertainty distributions shown in Fig. 4, analyzing the impact of batch size on failure detection for MCM, LVU and

ViLU on CC12M. We also provide two additional results with batch sizes of 16,384 and 32,768, showing that ViLU maintains strong failure detection capabilities even when the number of candidate captions is very large.

Batch Size	MCM [30]		LVU [8, 19, 47]		ViLU	
	AUC↑	FPR95↓	AUC↑	FPR95↓	AUC↑	FPR95↓
128	92.7	15.6	75.2	76.2	96.9	15.6
512	90.1	54.6	74.8	76.5	95.7	22.5
1024	88.8	58.8	74.4	76.5	95.2	25.2
2048	87.5	61.5	74.3	76.8	94.4	28.7
4096	86.4	64.2	73.9	77.0	93.6	31.8
8192	85.3	65.3	73.6	77.0	92.8	34.9
16384	84.5	66.4	73.3	76.7	91.9	37.8
32768	83.7	67.0	73.2	76.6	91.1	39.9

Table 7. Numerical results corresponding to Fig. 4, showing the effect of inference batch size on failure detection for ViLU (on CC12M).

C.3. Reliability of misclassification detection

Fig. 8 illustrates the relationship between misclassification detection performance and the zero-shot accuracy of the vision-language model for each baseline. Each dot at a given x-coordinate represents the classification performance of different baselines on the same dataset. The results emphasize the superior reliability of the uncertainty estimates provided by our method, particularly in low zero-shot accuracy settings. Notably, the tendency curves indicate a strong correlation between model performance and uncertainty metrics for both MCM and BayesVLM. Specifically, as zero-shot accuracy decreases, these two methods exhibit the worst performance. This suggests that they are only reliable when the model’s zero-shot accuracy is high—an unpredictable scenario in real-world settings, where ground-truth labels are unavailable.

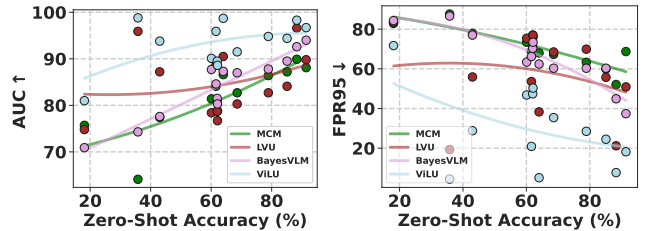


Figure 8. **Reliability of misclassification detection.** Our method, ViLU, enhances misclassification detection by providing more reliable uncertainty estimates, particularly when zero-shot accuracy is low.

C.4. Qualitative results

We provide additional visualizations on eight datasets in Fig. 9 and Fig. 10, illustrating the distribution of uncertainty scores for correctly and incorrectly classified validation samples. Our results demonstrate the consistency of ViLU in assigning high uncertainty scores to misclassified samples (red) and low uncertainty scores to correctly classified ones (blue).

Unlike visual uncertainty models such as ConfidNet [8], which rely solely on image features, our multimodal architecture leverages both visual and textual information to provide more reliable uncertainty estimates. Learning a cross-attention mechanism between image and text allows ViLU to better capture ambiguities in class definitions, leading to improved uncertainty calibration across diverse datasets.

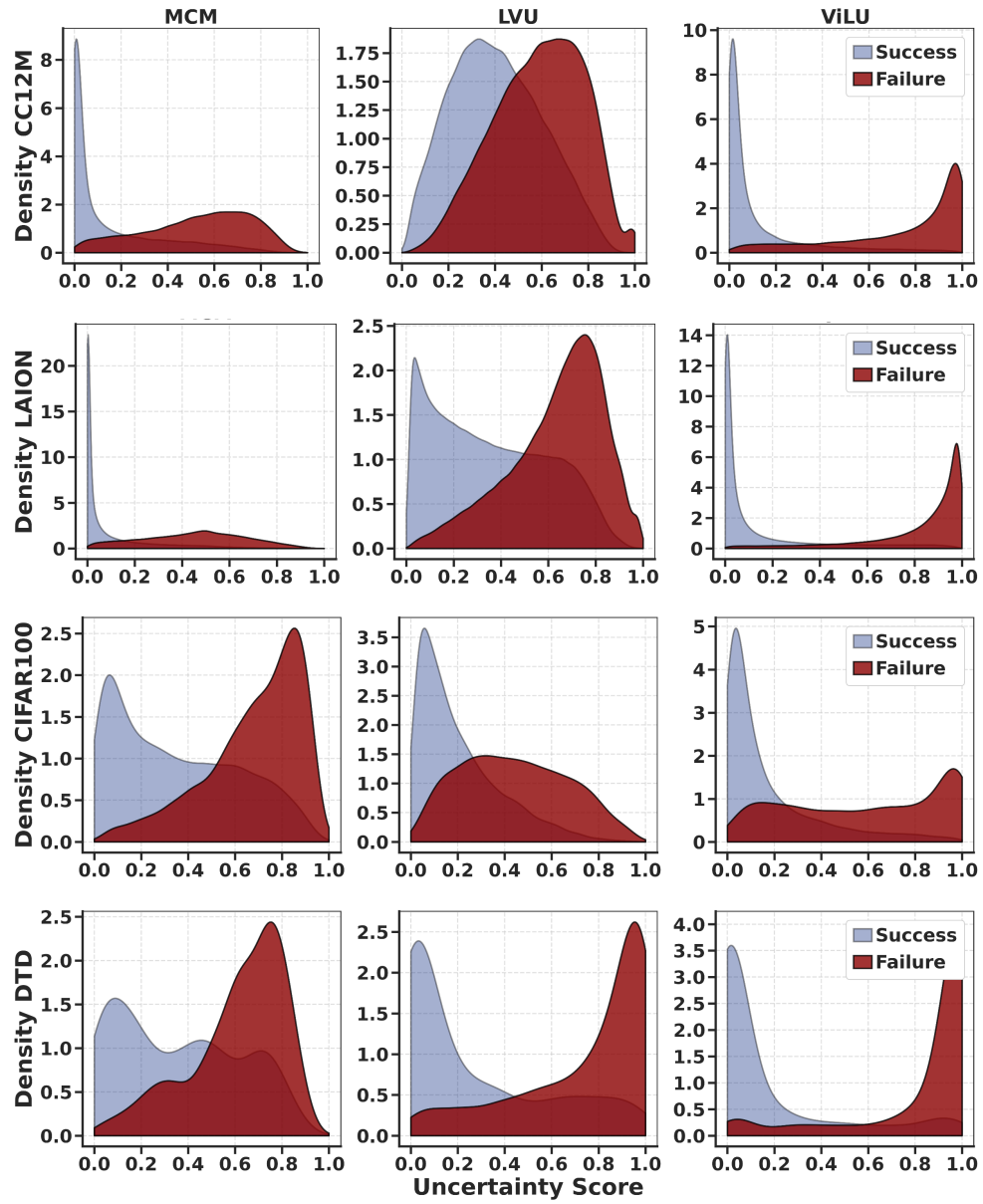


Figure 9. **Uncertainty score distribution.** Prediction for correctly and incorrectly classified samples on CC12M, LAION400M, CIFAR100 and DTD.

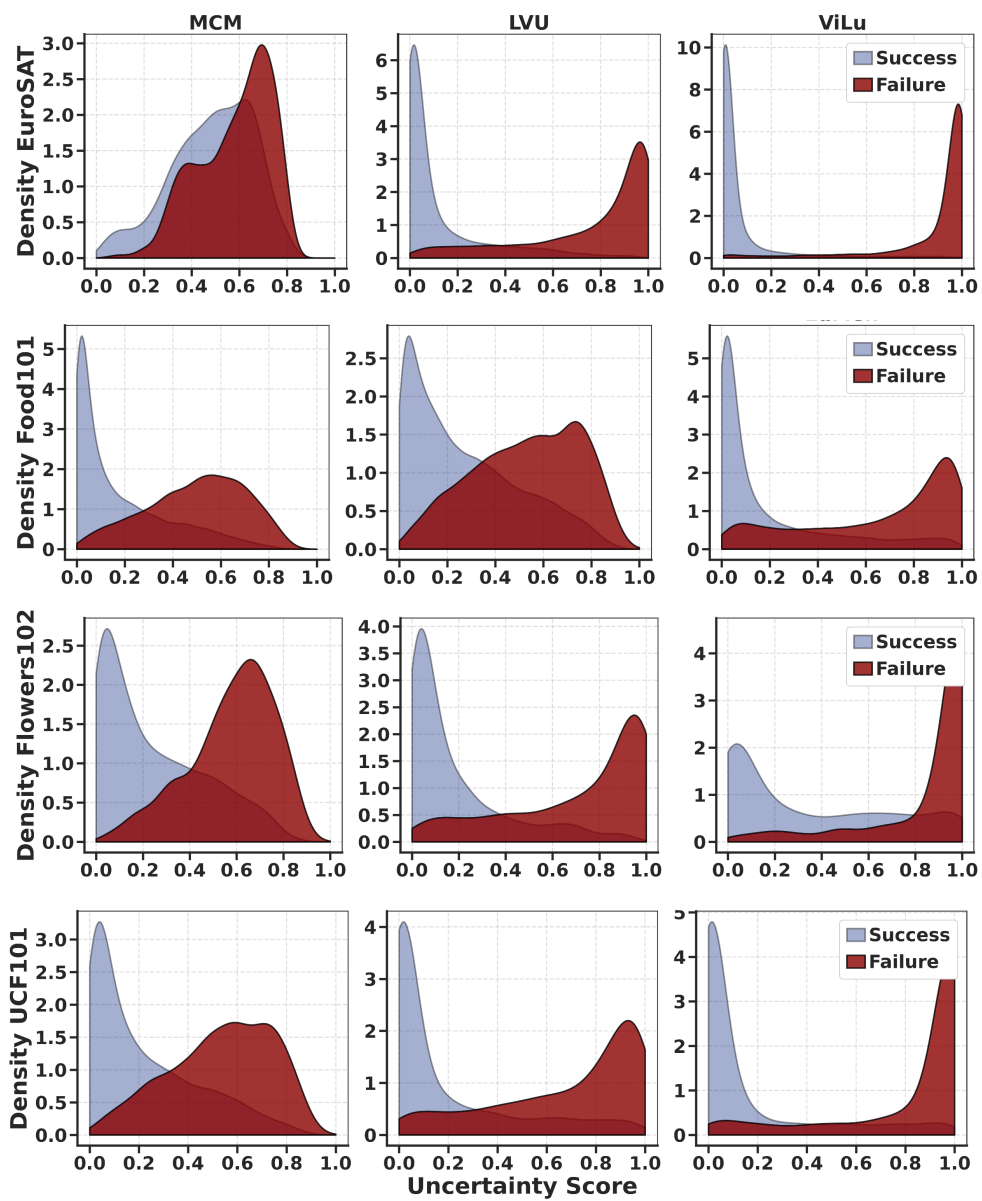


Figure 10. **Uncertainty score distribution.** Prediction for correctly and incorrectly classified samples on EuroSAT, Food101, Flowers102 and UCF101.